JCTC Journal of Chemical Theory and Computation

How Well Can Coarse-Grained Models of Real Polymers Describe Their Structure? The Case of Polybutadiene

Leonid Yelash,*,† Marcus Müller,‡ Wolfgang Paul,† and Kurt Binder†

Institut für Physik, WA 331, Johannes-Gutenberg Universität Mainz, Staudingerweg 7, D-55099 Mainz, Germany, and Institut für Theoretische Physik, Georg-August Universität Göttingen, Friedrich-Hund-Platz 1, D-37077 Göttingen, Germany

Received August 21, 2005

Abstract: Coarse-graining of chemical structure of macromolecules in the melt is investigated using extensive molecular dynamics simulation data which are based on a united atom force-field model of polybutadiene. Systematically increasing the number, *n*, of the united atoms approximated by an effective coarse-grained monomer, we study the influence of degree of coarse-graining on the structure functions such as the segment−segment intermolecular and intramolecular correlation functions. These results are compared to Monte Carlo simulations of the corresponding coarse-grained bead-spring model and Chen−Kreglewski potential for chain molecules. In contrast to the atomistic chemically realistic model of polybutadiene, the bending and torsional potentials are not included into the coarse-grained models. Nevertheless, for a range of intermediate values of *n* a good qualitative agreement between intra- and intermolecular coarse-grained correlations of the atomistic model and the coarse-grained bead-spring model is found on large and intermediate length scales, but deviations occur on length scales well below one nanometer. The structure functions obtained for the Chen−Kreglewski chains exhibit many artificial features.

1. Introduction

Understanding complex processes in real soft matter systems such as, e.g., relaxation processes in polymeric systems or the self-assembly and function of biological membranes is only possible with physically adequate and computationally effective models. Concerning different modeling approaches one can distinguish between microscopic, mesoscopic, and macroscopic models depending on the length and time scales of described objects and processes. At microscopic scales, the elementary degrees of freedom are due to atoms, and one deals with the intermolecular interactions and the atomistic structure of matter. Using molecular dynamics (MD) and Monte Carlo (MC) simulation methods,[1−4] one can obtain many properties, including the structure functions, which can be directly compared with corresponding experimental data. This microscopic structure in real systems can be experimentally probed by neutron or X-ray scattering.

The microscopic approaches require force-fields, which capture the nature of the different interactions. Some important types of interactions are the van der Waals (dispersion), polar, and ionic interactions. Accurate interatomic potential functions can be obtained from quantum chemical ab initio calculations of small molecules, e.g., using the Gaussian method. The force-field parameters can be also optimized in an automatic parametrization method[5] using experimental density and heat vaporization data of liquids. Such interaction potentials obtained for small molecules can also be used in atomistic simulations of oligomers and moderately long chains. In all-atom (AA) approaches,[4,6,7] for example, one explicitly describes all atoms in the simulation, e.g., the carbon atoms with the chemically bonded hydrogen atoms. However, this approach becomes inefficient for macromolecules, although it can be successfully applied to small and moderately large molecules. By ignoring hydrogen

* Corresponding author phone: +49-6131-3924104; e-mail: yelash@uni-mainz.de.
† Johannes-Gutenberg Universität Mainz.
‡ Georg-August Universität Göttingen.

10.1021/ct0502099 CCC: $33.50
Published on Web 02/04/2006

atoms in the united atom (UA) approach or by replacing the quantum mechanical potentials by computationally simpler functions such as the Lennard-Jones potential one can achieve an important improvement of the efficiency in computer simulations, i.e., a speedup of about 2 orders of magnitude in MD simulations. However, natural biological macromolecules as well as many polymers of industrial interest are usually consisting of several thousands up to some millions of atoms. A simulation of a microscopic UA model then often would require many more orders of magnitude of computer time to equilibrate the system than is available even on the fastest supercomputer. It is therefore necessary to explore more efficient computational techniques.

A promising approach, which can also increase the efficiency of simulations substantially and connect the microscopic and mesoscopic scales, is called "coarse-graining".[8−21] In this method one starts with a microscopic description of real molecules and reduces the degree of freedom, for example, by approximating several primary chemical units (e.g., carbon groups) by an effective monomer. Formally, a coarse-graining method can be related to the renormalization group approach for critical phenomena, in which an original Hamiltonian $H(\boldsymbol{x})$ of the system with $\boldsymbol{x}$ degrees of freedom has to be replaced by an effective Hamiltonian $F(\boldsymbol{m})$ with $\boldsymbol{m}$ coarse-grained degrees of freedom.[9,10] One tries to carry out a mapping[11−21] between the interactions on the atomistic scale and suitable effective interactions between the effective segments on the mesoscopic scale, attempting to create as much similarity between the physical properties of the atomistic model and the coarse-grained model as possible. Although this approach has had promising successes, it is clear that fine-scale structural details are lost, and as a consequence the desired physical properties of the system can only approximately be described. The question arises which level of coarse-graining is optimal, i.e., how many atoms (or united atoms, respectively) along the backbone of a chain should be combined into an effective segment. Some answers to this question can be found in the quoted literature, but they are still incomplete.

Similar approximations as in the coarse-graining method are used in deriving analytical models, where the details of atomistic structure of real molecules are usually neglected. In the first-order thermodynamic perturbation theory (TPT1),[22−25] for example, the theoretical monomer approximately represents several carbon groups of a real chain, e.g., alkanes.[26] In TPT1, a dimer consisting of two tangent spheres can model alkanes such as butane, which has four carbon groups. In a coarse-grained description one can tune the "resolution" of the model by merging different number of primary units. In this way it is possible to cover different physical scales bridging the gap between the micro- and mesoscopic scales. Hence, the coarse-graining approach is an extensively developed area of modern science dealing with molecular modeling.

Recently, the dissipative particle dynamics (DPD) method, which is a mesoscopic particle-based simulation technique intensively developed during the past decade,[27−30] has been applied to *cis*-polybutadiene.[31] In contrast to the standard molecular simulation techniques such as molecular dynamics and Monte Carlo, the particles in DPD represent a small amount of fluid which can include a large number of atoms. The DPD-particles interact via a soft-repulsive potential (a conservative force in DPD). In this method, however, it is still a difficult problem to relate the interactions of the DPD-particles to a microscopic interaction potential (which can be obtained from the first principles). A further step beyond DPD modeling of polymers is the soft-ellipsoid approach,[32] in which the volume occupied by a chain molecule is approximated by an ellipsoid.

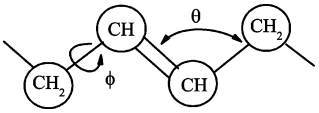

Figure 1. Schematic united atom (UA) model of polybutadiene molecules. The carbon groups of polybutadiene, which include one carbon atom and up to three hydrogen atoms (*CH*, CH_2, and endgroup CH_3), are approximated by spheres − the united atoms. The bond lengths between the united atoms are set to fixed values depending on the type of the bond: $r_0 = 1.34$ Å for $CH{=}CH$, $r_0 = 1.5$ Å for $CH{-}CH_2$ (α-bond), $r_0 = 1.53$ Å for $CH_2{-}CH_2$ (β-bond). The bending potential (eq 4) describes the bond angle θ which can harmonically change near the values 112° and 126° for $CH_2{-}CH_2{-}CH$ and $CH_2{-}CH{=}CH$, respectively. The torsional potentials (eq 5) describe the cis, gauche, and trans conformations, which can be distinguished by the torsion angle ϕ.

In this paper, we study the influence of the scale over which the coarse-graining is performed on the segment−segment correlation functions and the bond angle distribution of an atomistic UA model of polybutadiene.[33] We compare these results with Monte Carlo simulations of two coarse-grained models for chain molecules as an input. Polybutadiene has been chosen due to the availability of extensive molecular dynamic simulations[34−37] and experimental data.[35,36] Furthermore, a simple chemical structure and its importance for the chemical industry makes polybutadiene attractive to study.

2. Modeling Polybutadiene

2.1. United-Atom Model of Polybutadiene. The high-frequency motions, e.g., the hydrogen atoms vibrations, occur on very short time and length scales if compared to the typical scales for the molecular motions. An exact treatment of such motions can be very costly in computational simulations on long time scales. In a first step, one can approximate the entire functional group by one effective atom located at the position of the carbon atom. This effective group is then called united atom (UA). For example, each carbon group of polybutadiene, i.e., a carbon atom with bonded hydrogen atoms, can be replaced by one effective atom, which is shown schematically in Figure 1. Using this united atom model one can extend the investigation to longer time scales. Furthermore, there is a possibility to refine the results of the united-atom modeling later by reintroducing the neglected hydrogen atoms.

We use the united atom force field model of polybutadiene developed by Smith and Paul[33] which is based on the results of quantum chemical ab initio calculations. This model was

Table 1. Bond Lengths of Polybutadiene

bond type	bond length r_0 [Å]
CH═CH	1.34
CH−CH$_2$ (α)	1.5
CH$_2$*−CH*$_2$ (*β*)	1.53

extensively tested in many molecular dynamic simulations and has been shown to reproduce the experimental data for dielectric spectroscopy,[34] dynamic neutron scattering,[35] and relaxation processes[36] in polybutadiene melts very well.

The potential energy of polybutadiene can be written as a sum of the different contributions

$$U = U_{\text{bond}} + U_{\text{angle}} + U_{\text{tors}} + U_{\text{LJ}} \tag{1}$$

whereas U_{bond} is the bond length potential, U_{angle} is the bending energy for the angle between two neighboring bonds, U_{tors} is the energy of the torsion angles, and U_{LJ} is the Lennard-Jones interaction.

In the polybutadiene model, the bond lengths are rigid, and the distances between the carbon groups have been set to $r_0 = 1.34$, 1.5, and 1.53 Å for *CH═CH*, *CH*$_2$*−CH*, and *CH*$_2$*−CH*$_2$ bonds, respectively (see Table 1).

The potential energy of such bonds can be formally given by the Dirac's delta function

$$U_{\text{bond}}(r_{ij}) = C\delta(r_{ij} - r_0) \tag{2}$$

where the amplitude prefactor C is used here for dimensional reasons: $\delta(\mathbf{r})$ has dimension of inverse volume.

The bending contribution U_{angle} can be given by a harmonic deviation of the angle θ from an equilibrium angle θ_0

$$U_{\text{angle}}(\theta) = \frac{k}{2}(\theta - \theta_0)^2 \tag{3}$$

where θ is the angle between three bonded carbon groups. For computational reasons it is convenient to express the bending potential eq 3 in terms of cosθ:

$$U_{\text{angle}}(\theta) = \frac{k}{2\sin^2\theta_0}(\cos\theta - \cos\theta_0)^2 \tag{4}$$

For modeling polybutadiene, two bond angles were used: $\theta = 2.1973$ rad (125.9°) for the *CH*$_2$*−CH═CH*-type bonds and $\theta = 1.9487$ rad (111.6°) for the *CH*$_2$*−CH*$_2$*−CH*-type bonds.

The rotations around the bonds involve the torsional potential

$$U_{\text{tors}}(\phi) = \frac{1}{2}\sum_{n=1}^{6} k_n(1 - \cos n\phi) \tag{5}$$

where ϕ is the torsional angle (shown in Figure 5). The torsional potential is a four-particle potential. One can distinguish between five types of the chain conformations in polybutadiene: the cis- and trans-types double bonds *CH*$_2$*−CH═CH−CH*$_2$, the cis- and trans-types α-bonds *CH═CH−CH*$_2$*−CH*$_2$, and the *β*-bond *CH−CH*$_2$*−CH*$_2$*−CH*.

The interactions between the atoms which are arranged along the backbone of a chain at least four atoms away from each other or between the atoms of different chains are modeled via the Lennard-Jones potential:

$$U_{\text{LJ}}(r_{ij}) = \epsilon_{ij}\left[\left(\frac{\sigma_{ij}}{r_{ij}}\right)^{12} - 2\left(\frac{\sigma_{ij}}{r_{ij}}\right)^{6}\right] \tag{6}$$

The pair interaction parameters, ϵ_{ij} and σ_{ij}, which depend on the type of the interaction between the different carbon groups, can be found elsewhere[33,37] (see also Tables 1−4).

For our purpose we utilize the molecular dynamics simulation configuration trajectories of polybutadiene at atmospheric pressure obtained by Krushev[37] at temperatures 240 and 353 K, which are well above the glass transition temperature of polybutadiene $T_g \approx 180$ K. The simulation box consisting of 40 chains with 116 united atoms per molecule has the edge size 47.665 and 49.33 Å, which at these temperatures yields the polybutadiene density 0.9652 g/cm^3 and 0.8676 g/cm^3, respectively.

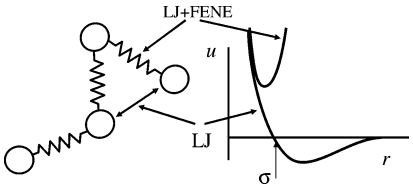

Figure 2. Bead-spring model for chain molecules based on the Lennard-Jones and FENE potentials. Circles represent the coarse-grained monomers. Springs represent the bonded interactions between monomers via the LJ+FENE potential. Nonbonded monomers interact via the Lennard-Jones potential. The corresponding potential curves are shown schematically on the right-hand side.

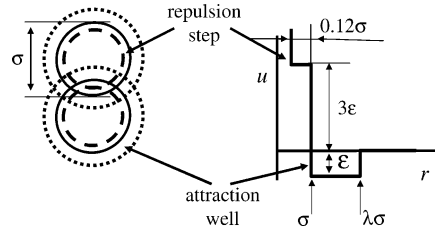

Figure 3. The Chen and Kreglewski interaction potential.[61] The solid circles represent the "softened" segment diameter σ, at which the molecules repel each other with interaction energy $+3\epsilon$. The interaction energy diverges at the hard-core diameter 0.88σ (dashed circles). The corresponding potential curve is shown on the right-hand side. For comparison, the interaction energy in the hard-sphere and square-well models diverges at diameter σ.

2.2. Coarse-Grained Bead-Spring Description of Polybutadiene. Coarse-grained models have been applied to different problems such as surfactant and lipid systems,[38−45] to study the self-organization of rod-coil molecules,[46] surfactant oligomers,[47] diblock copolymers,[48,49] chemically reacting systems,[50] nanoparticles,[51] liquid bisphenol A-polycarbonate,[15,16,21] and phospholipids.[52,53]

A widely utilized coarse-grained bead-spring model has been developed by Kremer and Grest.[54] The Lennard-Jones potential describes the repulsion and dispersion forces

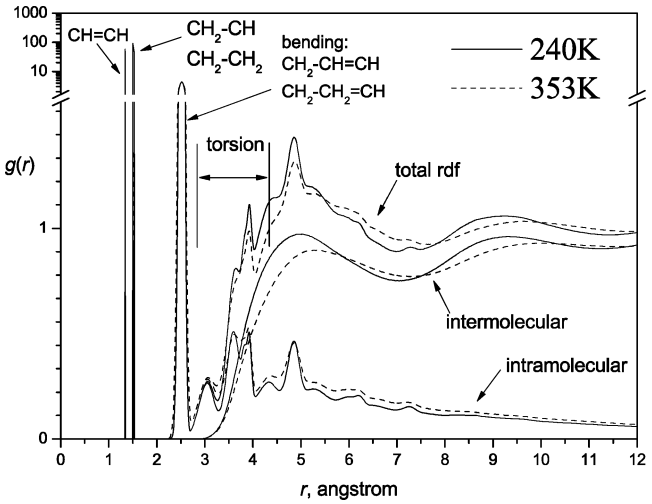

Figure 4. Segment−segment correlation functions from atomistic simulations of polybutadiene at 240 K (solid) and 353 K (dashed) and atmospheric pressure.[37] The intramolecular correlations are the segment−segment correlations along a polymer molecule. The intermolecular correlations are the correlations of segments which belong to different molecules. The total radial distribution function is a sum of the intra- and the intermolecular functions. The sharp (δ-function-like) peaks at $r = 1.34$, 1.5, and 1.53 Å correspond to the double (*CH═CH*) and single (*CH*$_2$−*CH* and *CH*$_2$−*CH*$_2$) bonds of polybutadiene. The correlation peak at $r \approx 2.53$ Å represents the distribution of the united atoms interacting via the bending potential (eq 4). Several correlation peaks at 3 Å $\leq r \leq$ 4 Å are due to the torsional cis and trans interactions (bonding four carbon groups along a backbone).

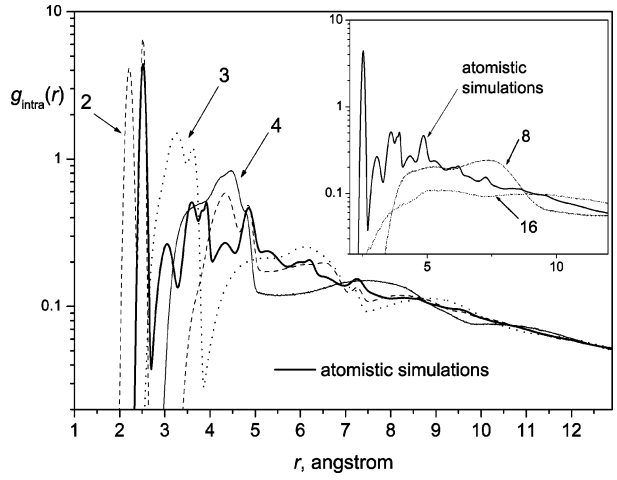

Figure 5. Coarse-graining of the intramolecular segment−segment correlation function of polybutadiene (240 K). The numbers are for the different degrees of the coarse-graining. A bold curve is the correlation function calculated using the UA MD data[37] (also shown in Figure 4, however, the δ-type peaks at $r = 1.34$ Å, 1.5 Å, 1.53 Å are omitted here).

between the segments for both the intermolecular and nonbonded intramolecular interactions:

$$U_{\mathrm{LJ}}(r) = 4\epsilon\left[\left(\frac{\sigma}{r}\right)^{12} - \left(\frac{\sigma}{r}\right)^{6}\right] + \frac{127}{4096}\epsilon \qquad (7)$$

The interaction range of the Lennard-Jones potential is infinite. In the simulations, however, it is computationally effective to reduce the interaction range of the potential, which does not change the qualitative phase behavior.[55] In the literature one can find different ways how to truncate the interaction range of the potential. In this work we use a cutoff at $r_{\mathrm{cutoff}} = 2\sqrt[6]{2}\sigma$,[56,57] which is close to the minimum of the pair correlation function beyond the second correlation shell in the dense phase, thus minimizing the error of cutoff. The potential is also shifted (by the last term in eq 7) in order to avoid an energy discontinuity at the cutoff distance.

Table 2. Bending-Potential Parameters of Polybutadiene

type	energy k [K]	angle θ_0 [rad]
CH$_2$−*CH*$_2$−*CH*	57899	1.9487
CH$_2$−*CH═CH*	45010	2.1973

The interactions of the segments bonded along a backbone are modeled via the FENE potential in addition to the Lennard-Jones potential. FENE stands for finitely extensible nonlinear elastic. This model is shown schematically in Figure 2. In the coarse-grained bead-spring model, the distance between the bonded segments can change to a certain extent, e.g., upon variation of the pressure, yielding an equilibrium distribution of bond lengths for fixed thermodynamic parameters. The stretching of the bonds is restricted by a bond-energy penalty, which diverges at the bond length $r = 1.5\sigma$:

$$U_{\mathrm{FENE}}(r) = -33.75\epsilon \ln\left[1 - \left(\frac{r}{1.5\sigma}\right)^2\right] \qquad (8)$$

With this choice of the constants in the FENE potential the maxima of the distance distribution for the bonded and nonbonded monomers in a dense melt occur at $r \approx 0.96\sigma$ and $r \approx 1.1\sigma$, respectively. The parameters of the Lennard-Jones, bond length and bending potentials can be further optimized using results of the atomistic simulations and experimental data to reproduce the observables.[58] An optimization of the bond angle parameter can be important to reproduce, for example, the peaks of the pair correlation function.[59] For modeling flexible macromolecules of polybutadiene on the coarse-graining level no bending potential (which is the coarse-grained analogue of the angular potential eq 4) is included here, unlike for the modeling of lipids and surfactants.

This bead-spring model is very well studied and has already been applied to many different problems including, recently, the coarse-grained modeling of polymer solutions.[56,57,60] For example, it has been shown that phase behavior predicted by this model for mixtures of carbon dioxide/hexadecane is in good agreement with experimental data.

2.3. Chen−Kreglewski Potential for Chain Molecules. Another coarse-grained model of chain molecules which we study here is based on the Chen−Kreglewski (CK) potential.[61] This interaction potential is the theoretical basis of some analytical equations of state such as BACK[61] and PC-SAFT[62,63] equations. The "softened" repulsion introduced into the Chen−Kreglevski potential is also used in the SAFT equation.[26] The potential is shown schematically in Figure

Table 3. Torsion-Potential Parameters of Polybutadiene[37]

type	k_1 [K]	k_2 [K]	k_3 [K]	k_4 [K]	k_5 [K]	k_6 [K]
$CH_2-CH=CH-CH_2$ (cis or trans)	0	12083.3	0	0	0	0
$CH=CH-CH_2-CH_2$ (α- cis)	432.984	−20.1388	584.025	80.5552	191.319	−60.4164
$CH=CH-CH_2-CH_2$ (α- trans)	−120.833	−367.533	1198.26	40.2776	45.3123	−30.2082
$CH-CH_2-CH_2-CH$ (β)	−498.435	−312.151	−2034.02	−35.2429	−125.868	−95.6593

Table 4. Lennard-Jones Parameters of Polybutadiene

interaction type	energy ϵ [K]	diameter σ [Å]
$CH \leftrightarrow CH$	50.347	3.8
$CH \leftrightarrow CH_2$	51.102	4.257
$CH_2 \leftrightarrow CH_2$	47.125	4.5

3. It is similar to the square-well potential; however, it has an additional repulsive step (inverse well):

$$U_{CK}(r) = \begin{cases} +\infty & : \quad r < \sigma - 0.12 \\ +3\epsilon & : \quad \sigma - 0.12 < r < \sigma \\ -\epsilon & : \quad \sigma < r < \lambda\sigma \\ 0 & : \quad \lambda\sigma < r \end{cases} \tag{9}$$

The height $+3\epsilon$ and the width 0.12σ of the repulsion step were empirically determined by Chen and Kreglewski in order to improve the description of the equation of state for some small molecules, e.g., noble gases and short alkanes.[61] Here we study the structure which can be obtained for a dense melt in computer simulations using the Chen−Kreglewski potential and compare these results to those from the coarse-grained bead-spring model and from the atomistic simulations. For modeling chain molecules using the Chen−Kreglewski potential, the monomers are connected by rigid bonds as it is assumed in many analytical theories for the equations of state.

2.4. Simulation Details. The Monte Carlo simulations of the coarse-grained bead-spring model and the Chen−Kreglewski potential are performed using the computer code which has been developed in the Condensed Matter Theory Group at the University of Mainz for the Lennard-Jones+FENE model[64] and generalized to different interaction potentials.[65,66] For these potentials we generate chains with $m = 29$ beads per molecule. This number of monomers represents a 4:1 mapping of an atomistic polymer with 116 united atoms per chain onto the coarse-grained chain molecules. This mapping ratio has been found to be an optimal degree of the coarse-graining for polybutadiene, which we discuss later on in this paper. In the simulations of the LJ+FENE chains, the simulation cell contains 160 chain molecules. For the CK model we use 40 chains per cell. Initial configurations of the chain systems are generated using the configurational bias method.[1] After equilibrating the chains, the MC simulations are performed in an *NpT* ensemble, in which in addition to volume change (once per MC step) we include the local displacement of randomly chosen monomers (every monomer once per MC step) as well as "reptation moves"[67] where a monomer at one end of the chain, which is chosen randomly, is cut off and added at the other end of the same molecule (typically 100 attempts per MC step).

The choice of the reduced temperature and pressure can have a significant influence on the local packing of the monomers in the coarse-grained simulations.[68] Unfortunately, it is not possible to simply utilize the values of the molecular interaction parameter, ϵ, from a united atom model for a coarse-grained one since due to a different representation of the structure on the length scale of few monomers the energy scales of these modeling approaches can be different by 1 order of magnitude: In the atomistic model, the monomers are bonded at distance $r_0 \approx 1.5$ Å overlapping strongly and forming a kind of flexible tube of the diameter ≈4.5 Å. In the coarse-grained model, a bead accounts for all possible interactions of approximated united atoms with other ones; therefore, the interaction energy of a bead is an average interaction energy, which is very different from that in the united atom model.

The reduced temperature and pressure for the coarse-grained simulations are obtained using the results of our recent investigation of phase diagrams of chain molecules[65,66] which is based on Monte Carlo simulations, analytical equations of state, and experimental data of polybutadiene. The correlation of the experimental data of polybutadiene at temperatures between 300 and 460 K and pressures from the atmospheric one to 200 MPa has yielded an estimate of $\epsilon/k_B \approx 269$ K and $\sigma = 3.4$ Å, from which one can calculate reduced temperatures $T^* = 240\ \text{K}/(\epsilon/k_B) \approx 0.892$ and $T^* = 353\ \text{K}/(\epsilon/k_B) \approx 1.312$ and reduced pressure $p^* = 10^5\ \text{Pa}\cdot(\sigma^3/\epsilon) \approx 1.06\cdot10^{-3}$. Hence, the coarse-grained systems are simulated here at the reduced temperatures $T^* \equiv k_BT/\epsilon = 0.9$ and 1.3 and reduced pressure $p^* \equiv p\sigma^3/\epsilon = 0.001$ yielding very similar thermodynamic states (i.e., a melt at ambient pressure and temperature) for both the atomistic and the coarse-grained models. The reduced monomer density, $\rho^* \equiv \rho\sigma^3$, obtained at these temperatures is 0.893 and 0.781 in LJ+FENE and 0.863 and 0.789 in CK simulations, respectively.

3. Results and Discussions

3.1. Pair Correlation Functions of Polybutadiene. The segment−segment correlation functions calculated from the united atom molecular dynamics simulation data of polybutadiene[37] are shown in Figure 4. The detailed structure revealed in this figure represents different kinds of interactions between functional groups of polybutadiene and different energy scales for these interactions, if compared to the thermal fluctuations at the simulated conditions. At 240 K the structure is more pronounced (compare the height of the minima and maxima of $g(r)$) and more compact (compare r at the extremes) than at 353 K. It is convenient to separately investigate the segment−segment correlations for monomers which belong to the same backbone (intramolecular) and to

different molecules (intermolecular). The total segment−segment correlation function is the sum of the intra- and intermolecular functions.

At first, we analyze the intramolecular correlations. The three peaks at distances $r = 1.34$, 1.5, and 1.53 Å correspond to the covalent bonds between the carbon groups: *CH═CH* (double bonds), CH_2-CH (α-bonds), and CH_2-CH_2 (β-bonds), respectively. Of course, these sharp peaks are a somewhat artificial feature of the fixed bond length constraint used in the simulation. A more realistic description allowing for a more accurate potential for the length of the covalent bonds would result in peaks of finite (albeit small) width. Therefore it is not relevant to keep such features for a coarse-grained modeling. The fourth peak at distance $r = 2.53$ Å is somewhat broader due to the bending potential eq 4 which restricts the relative positions of the next-nearest-neighbor carbon groups along the backbone. Several peaks between $r = 3$ Å and $r = 4$ Å are due to the four-body interactions which are modeled by the torsional potential eq 5 in the simulation.[37] At large length scales, the intramolecular correlation function becomes smoother as the monomer positions become uncorrelated and decays on the length scale of the molecular extension.

The intermolecular correlation functions of polybutadiene, which are also shown in Figure 4, exhibit the main peak at distance $r \approx 5$ Å, a wide correlation hole at $r \leq 3$ Å caused by the excluded volume interaction of the Lennard-Jones potential and typical oscillations for long length scales. The intermolecular pair correlation function is much smoother than for the intramolecular one because the nonbonded interactions described by the Lennard-Jones interactions are much softer.

3.2. Coarse-Graining of the Atomistic Model. Here we investigate how the correlation functions develop if several united atoms of the atomistic model are replaced by one effective segment. Our aim is to find out the number, *n*, of united atoms taken to correspond to one effective segment which yield an optimal coarse-grained representation within the bead-spring model, in the sense that similar conditions are obtained. We denote *n* as a "degree of coarse-graining" in the following. Since there is no unique way of mapping a polymer molecule onto a coarse-grained molecule we calculate the average positions of centers of mass without accounting for the molecular masses of different carbon groups, i.e., *CH*, CH_2, and CH_3 are equivalently treated in our approach.

Figure 5 shows the intramolecular correlation functions obtained in the atomistic simulations of polybutadiene at 240 K and atmospheric pressure as well as for different coarse-graining degrees, *n*, given by the numbers in the figure. One can see that different choices for *n* have different impact on the structure. For low degree of coarse-graining (e.g., $n = 2$ and 3), additional peaks appear which are not present in the atomistic structure. At high degree of coarse-graining ($n \geq 8$ shown in the inset), the structure is nearly uniform, and correlations can also be found on length scales shorter than the size of the coarse-grained segments due to the overlapping of the effective segments.

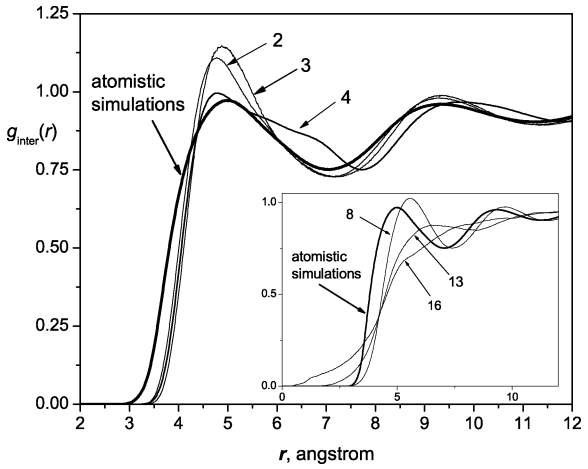

Figure 6. Coarse-graining of the intermolecular segment−segment correlation function of polybutadiene at 240 K. For $n \leq 8$, the correlation function changes quantitatively. For larger degrees of the coarse-graining (e.g., $n > 13$), the correlation peaks and minima disappear and the correlation hole at $r < 3$ shrinks. A bold curve is the correlation function calculated using the UA MD data[37] (also shown in Figure 4).

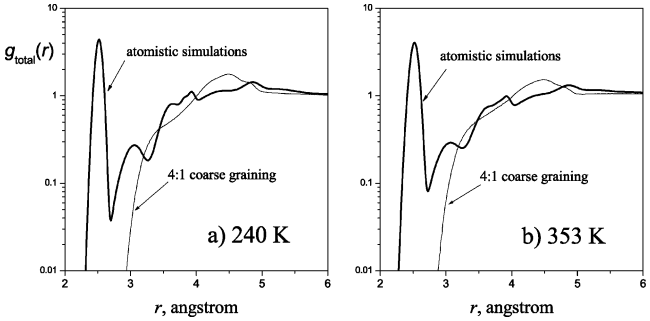

Figure 7. Total segment−segment correlation functions of polybutadiene for the optimal value $n = 4$ of the coarse-graining degree (thin curve). Bold curves are the correlation functions calculated using the UA MD data[37] shown in Figure 4.

The intermolecular correlations are less sensitive to the coarse-graining for small values of *n*, in contrast to the intramolecular correlations. In Figure 6 one can see that the intermolecular correlation function only slightly changes for $n < 4$. At first, the intermolecular correlations in the first correlation shell (the peak at $r \approx 4.5$ Å) increase due to the loss of local internal structure. For the coarse-graining degree $n = 4$, the intermolecular structure becomes nearly the same as in the atomistic model. In this approximation, butadiene, which is the monomer of polybutadiene, is replaced by one effective monomer. For a larger degree of coarse-graining, the structure decreases, and we can observe the fusion of the effective segments (e.g., for $n = 16$, $g(r)$ becomes nonvanishing down to $r = 0$).

The total correlations function for the optimal choice, $n = 4$, of the coarse-graining degree is shown together with the atomistic total correlations function in Figure 7. Although, the correlation functions change with temperature, this effect is not very strong for polybutadiene at 240 K to 353 K in contrast to the variation of *n*, which has a much stronger impact on the structure functions. One can conclude that for

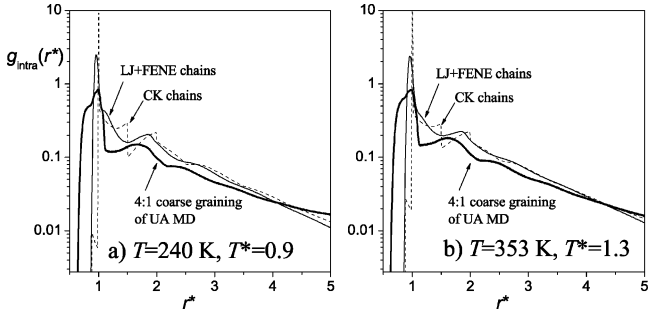

Figure 8. Intramolecular segment−segment correlation functions obtained from the Monte Carlo simulations of the LJ+FENE bead-spring chains (thin solid curve) and the Chen−Kreglewski chains (dashed curve) for chains with 29 beads/molecule at reduced pressure $p^* \equiv p\sigma^3/\epsilon = 0.001$ and reduced temperatures $T^* = 0.9$ and 1.3. Bold curves are from the UA MD simulations of polybutadiene[37] at 240 and 353 K. (The bold curve in (a) is the curve 4 in Figure 5; however, here the distance $r^* = r/\sigma$ has been scaled by the effective Lennard-Jones diameter $\sigma = 4.5$ Å.)

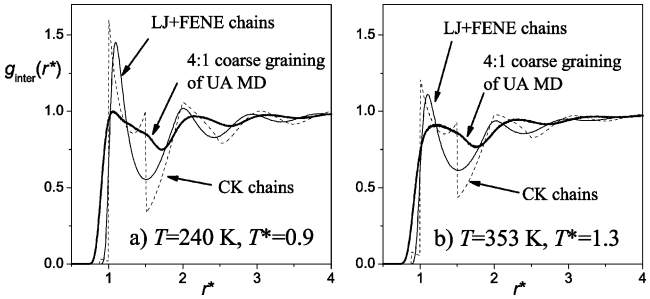

Figure 9. Intermolecular pair correlation functions obtained from the Monte Carlo simulations of the bead-spring chains (thin solid curves) and Chen−Kreglewski chains (dashed curves) for the same systems as in Fugure 8. Legends as in Figure 8.

the pair correlation functions there is an optimal value of the coarse-graining degree beyond which the intermolecular structure simplifies drastically and the intermolecular correlations nearly vanish. In this limit the polymer melt is described as if it would result from an ensemble of noninteracting ideal random walks, i.e., the well-known Flory picture of dense polymer melts. On this extremely simplified level of the description, all effects of chemical detail would be lost. In the case of polybutadiene studied here this value of n when correlations are essentially lost is between 8 and 16, which corresponds to approximation of three to four monomers (butadiene) by one effective segment. Too small values of coarse-graining degree, however, can produce unphysical correlations such as curve 3 in Figure 5.

3.3. Structure of LJ+FENE and CK Chains. Discontinuous potentials, e.g., the hard sphere and square-well potentials, are widely used in statistical theories of molecules. The reason for using such simplified potentials is, of course, not a better representation of the physics of molecular interactions in real substances by such models but is rather pragmatic and dictated by the complexity of molecular theories which have to deal, for example, with multiple integration of the potential functions. Even for simple potentials these theories frequently can only be solved in analytical form using several approximations. However, such a discontinuity of the steplike potential influences the structure of fluids.

In Figure 8 the intramolecular segment−segment distribution functions are compared for the Chen−Kreglewski and the LJ+FENE potentials for chain molecules with $m = 29$ monomers/chain at two temperatures. This number of monomers corresponds to the 4:1 coarse-graining of the atomistic simulation data of polybutadiene (bold curve in the figure). The molecular parameters, ϵ and σ, and the reduced state parameters, $p^* = 0.001$ and $T^* = 0.9$ and 1.3, are chosen the same for the CK and LJ+FENE potentials.

At two temperatures the overall agreement for the intramolecular correlation functions from the coarse-grained and atomistic models does not change significantly: Some change of the structure occurs on length scales between $r^* = 1$ and $r^* = 2$ (i.e., in the range of the potential attractive part). However, there are significant qualitative differences in the correlation functions of the LJ+FENE (thin solid) and CK (dashed) models. The distribution functions from the LJ+FENE potential and the UA MD simulations are smooth and continuous in the whole range of molecular distances, as one would expect. However, the Chen−Kreglewski model exhibits steplike jumps in the intramolecular correlations at several distances: at $r^* = 0.88$ due to the excluded volume interactions with a repulsive step, at $r^* = 1.5$ and $r^* = 2$ due to the square-well attraction and a strong peak at $r^* = 1$ (the bond length). Such peaks have been already observed in the atomistic simulations (Figure 4), which correspond to the nearly unchanged bond lengths between the carbon groups in real polymers. For the CK chains, however, this peak is due to the implementation of rigid bonds between the coarse-grained segments. The LJ+FENE model exhibit a continuous, smooth maximum at bond distances ($r^* \approx 0.96$). This peak can rather well be compared with the peak in the coarse-grained structure of polybutadiene (bold curve), although the last one is lower and broader.

The intermolecular correlation functions for the LJ+FENE and CK potentials are compared with the 4:1 coarse-graining of the atomistic data in Figure 9. The CK correlation function (dashed) shows similar discontinuities as discussed above for the intramolecular correlation function. The LJ+FENE correlation function (thin solid) yields a correct qualitative description of the 4:1 coarse-grained atomistic correlation function (bold curve in the figure), although the LJ+FENE structure is more pronounced. At higher temperature, the agreement improves because the height of the LJ+FENE main peaks decreases, and it approaches the atomistic one.

3.4. Bond Angle Distributions from Atomistic Modeling. The atomistic simulations yield the distribution of the bond angle with two very pronounced peaks at 112° for the CH_2-CH_2-CH groups and 126° for the $CH_2-CH=CH$ groups. This distribution decreases rapidly for other values of the bond angle. Figure 10 shows this bond angle distribution calculated from the atomistic simulation data for polybutadiene at 240 and 353 K and how this distribution changes if several carbon groups are approximated by an effective segment (for the 240 K curve). For increasing degree of coarse-graining, the peaks shift to higher values

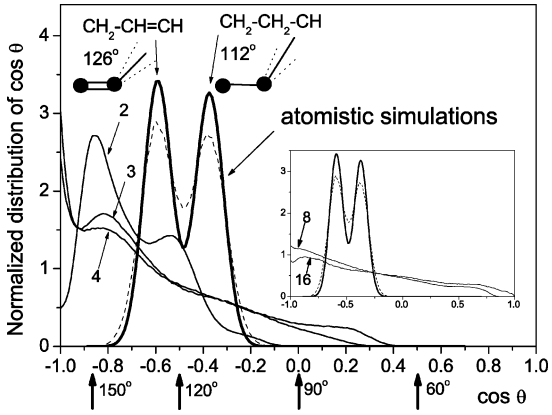

Figure 10. Bond-angle distribution of polybutadiene at 240 K (bold) and 353 K (dashed) and atmospheric pressure obtained using the UA MD simulation data.[37] The atomistic simulations at two temperatures yield qualitatively similar distributions with two peaks at $\theta \approx 112°$ and $\theta \approx 126°$ for CH_2-CH_2-CH and $CH_2-CH=CH$ groups, respectively. These distributions change significantly for the coarse-grained models (numbered curves). For clarity, only the coarse-grained results for 240 K are shown. The 4:1 curve for 353 K is shown in Figure 12.

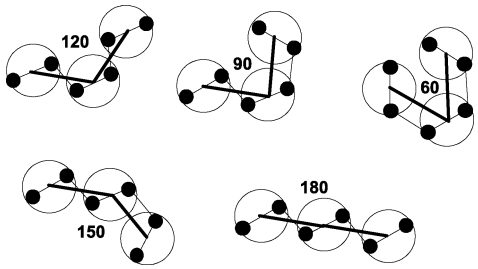

Figure 11. Schematic examples illustrating the bond angles which can be found for effective chains in a coarse-grained model if in the atomistic model only one bond angle is allowed (for instance, the bond angle 120° between the connected filled circles). Bold lines connecting the centers of the big, open circles are bonds in a coarse-grained model.

of the bond angle and the structure becomes smeared-out. For a coarse-graining degree $n > 4$ (i.e., if several butadiene groups of polybutadiene are approximated by one monomer), the peaked structure cannot be recognized any more in the coarse-grained model. The bond angle distribution becomes nearly uniform in the whole range of bond angle values. Figure 11 schematically illustrates that different bond angles can arise in a coarse-grained model even if in an atomistic model only one bond angle exists. For $n = 4$, which we so far identified as the best choice for the degree of coarse-graining, a residual structure at $\theta \approx 150°$ is, however, clearly visible in the angle distribution function in Figure 10. This means that on this coarse-graining level an effective bending potential should be used in simulations trying to describe polybutadiene, as in case of polyethylene.[69]

3.5. Bond-Angle Distributions from the LJ+FENE and CK Models. For simplicity, the coarse-grained models employed for the investigation here do not include explicitly a bending interaction potential, which however can be very important, for example, in the modeling of polymer crystallization.[69] As further motivation for this omission we note that in the first-order thermodynamic perturbation theory of Wertheim the chain molecules are modeled by flexible chains of tangent spheres. The stiffness of the molecules is considered as a second-order contribution to the free energy and is ignored in that analytical theory of chain molecules. To estimate the impact of simplifications due to ignoring the stiffness, the bond angle distribution is investigated here for polymer molecules.

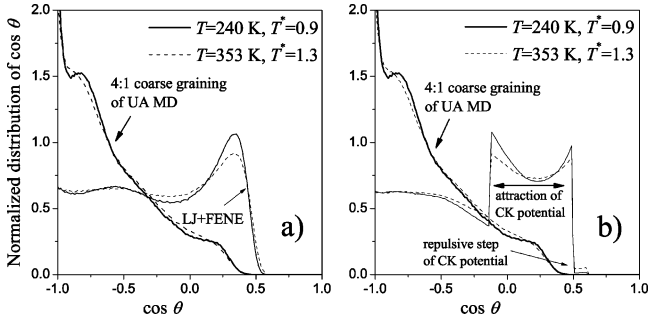

Figure 12. (a) Bond-angle distributions obtained in the Monte Carlo simulations of the bead-spring chains with 29 beads/molecule at reduced temperatures $T^* = 0.9$ (solid) and $T^* = 1.3$ (dashed) and reduced pressure $p^* = 0.001$. The 4:1 coarse-grained UA MD simulations of polybutadiene are at 353 K (dashed) and 240 K (solid, this is curve 4 in Figure 10). (b) Same as (a) but for the Chen−Kreglewski potential instead of the bead-spring potential. Although, no bending interaction is explicitly included in the coarse-grained LJ+FENE and CK simulations, the distributions of the bond angles become very inhomogeneous due to the excluded volume interactions.

The bond angle distributions for the coarse-grained LJ+FENE and Chen−Kreglewski potentials are compared in Figure 12 with the distribution functions obtained for the 4:1 coarse-graining of the UA MD data of polybutadiene at two temperatures. The bending interaction in polybutadiene is explicitly accounted for in the underlying atomistic model. The LJ+FENE bond angle distribution is nearly homogeneous over a wide range of large values of the bond angle. At $\theta \approx 70°$ ($\cos\theta_0 \approx 0.33$), it exhibits a maximum and vanishes rapidly for smaller bond angles. Hence, one can speak about stiffness of the LJ+FENE molecules with the equilibrium angle $\theta_0 \approx 70°$, although no bending potential has been included in the simulations. From the examination of the correlation hole and the main peak in Figures 8 and 9 one concludes that these are effects of the excluded volume interaction, which is explicitly present in the LJ+FENE potential.

The bond angle distribution for the Chen−Kreglewski chains exhibits steplike discontinuities similar to those discussed in detail for the pair correlation functions. It is worth mentioning here that in contrast to the bead-spring model the CK angle distribution jumps to zero for small values of the bond angle ($\theta \approx 52°$), which is due to the hard sphere repulsion in the CK potential. For the LJ+FENE model, this property decreases smoothly. Furthermore, there is a minimum of the CK distribution function at $\theta \approx 76°$ ($\cos\theta \approx 0.24$), which yields two equilibrium bond angles at $\theta \approx 96°$ ($\cos\theta \approx -0.1$) and $\theta \approx 62°$ ($\cos\theta \approx 0.47$). This

artifact is caused by the square-well attraction. The LJ+FENE potential yields a distribution function with one maximum and, hence, with only one equilibrium bond angle at $\theta_0 \approx 70°$.

4. Conclusions

Mapping of an atomistic model of polymers onto a coarse-grained one is a popular step to tackle the problem of bridging in structure from the subangstrom scale to mesoscopic scales, involving at the same time a considerable speed-up of the simulation codes. However, such a mapping necessarily is somewhat approximate, some information is necessarily lost, and the question arises at which level of coarse-graining one obtains the most reasonable compromise between atomistic accuracy and simulational efficiency. This is addressed in the present paper by a systematic comparison between different levels of coarse-graining.

We conclude that there is a reasonable correspondence, at least for the static structure functions, between correlations of LJ+FENE chains and suitable coarse-grained atomistic models, e.g., the coarse-graining degree $n = 4$ for polybutadiene, i.e., when 4 united atoms yield one effective subunit. Further investigations, for example, including dynamics, would be of great interest in order to complete the understanding of the coarse-graining effect on different properties.

In contrast, the Chen−Kreglewski model for chain molecules yields many artificial features in their correlations which have no counterpart in reality. As is well-known, the CK model is widely used mostly as a starting point for the approximate equation-of-state theories such as PC-SAFT. However, our recent analysis of this theory has revealed a variety of artifacts such as artificial gas−gas and liquid−liquid equilibria causing also systematic deviations between the equation of state and real data in regime of experimental interest,[65,66] while other theories based on the LJ+FENE potential exhibit a much better description of chain molecules. Therefore, we suggest abandoning the discontinuous potentials such as the CK potential as a starting point for the description of polymers.

Acknowledgment. We benefited from stimulating discussions with H. Weiss, U. Nieken, W. Hültenschmidt, Ch. Ch. Liew, A. Moreira, and O. Evers (all BASF Aktiengesellschaft, Ludwigshafen). We thank P. Virnau (MIT, Cambridge) for providing us with the Monte Carlo LJ+FENE code and for interesting discussions. CPU time was provided by the computing center of the Johannes-Gutenberg University of Mainz.

References

(1) Frenkel, D.; Smit, B. *Understanding Molecular Simulation: From Algorithms to Applications;* Academic Press: 2002.

(2) Allen, M. P.; Tildesley, D. J. *Computer simulation of liquids;* Clarendon Press: Oxford, 1991.

(3) Landau, D. P.; Binder, K. *A Guide to Monte Carlo Simulations in Statistical Physics;* Cambridge University Press: Cambridge, 2000.

(4) *Simulation Methods for Polymers*; Kotelyanskii, M., Theodorou, D. N., Eds.; Marcel Dekker: New York, 2004.

(5) Faller, R.; Schmitz, H.; Biermann, O.; Müller-Plathe, F. *J. Comput. Chem.* **1999**, *20*, 1009−1017.

(6) Polson, J. M.; Frenkel, D. *J. Chem. Phys.* **1999**, *111*, 1501−1510.

(7) Das, C.; Frenkel, D. *J. Chem. Phys.* **2003**, *118*, 9433−9440.

(8) Nielsen, S. O.; Lopez, C. F.; Srinivas, G.; Klein, M. L. *J. Phys.: Condens. Matter* **2004**, *16*, R481−R512.

(9) Paul, W. A Mapping from Atomistic Polymer Models to Coarse-Grained Models. In *Multiscale Computational Methods in Chemistry and Physics*; Brandt, A., Bernholc, J., Binder, K., Eds.; IOS Press: 2001.

(10) Binder, K.; Paul, W.; Santos, S.; Suter, U. W. Coarse-Graining Techniques. In *Simulation Methods of Polymers*; Kotelyanskii, M., Theodorou, D. N., Eds.; Marcel Dekker: New York, 2004.

(11) Paul, W.; Binder, K.; Kremer, K.; Heermann, D. W. *Macromolecules* **1991**, *24*, 6332−6334.

(12) Tries, V.; Paul, W.; Baschnagel, J.; Binder, K. *J. Chem. Phys.* **1997**, *106*, 738−748.

(13) Rapold, R. F.; Mattice, W. L. *Macromolecules* **1996**, *29*, 2457−2466.

(14) Doruker, P.; Mattice, W. L. *Macromolecules* **1997**, *30*, 5520−5526.

(15) Tschöp, W.; Kremer, K.; Batoulis, J.; Bürger, T.; Hahn, O. *Acta Polym.* **1998**, *49*, 61−74.

(16) Tschöp, W.; Kremer, K.; Batoulis, J.; Hahn, O.; Bürger, T. *Acta Polym.* **1998**, *49*, 75−79.

(17) Baschnagel, J.; Binder, K.; Doruker, P.; Gusev, A. A.; Hahn, O.; Kremer, K.; Mattice, W. L.; Müller-Plathe, F.; Murat, M.; Paul, W.; Santos, S.; Suter, U. W.; Tries, V. *Adv. Polym. Sci.* **2000**, *152*, 41−156.

(18) Kremer, K.; Müller-Plathe, F. *MRS Bull.* **2001**, *26*, 205−10.

(19) Hahn, O.; delle Site, L.; Kremer, K. *Macromol. Theory Simul.* **2001**, *10*, 288−303.

(20) Müller-Plathe, F. *ChemPhysChem* **2002**, *3*, 754−769.

(21) Abrams, C. F.; Kremer, K. *Macromolecules* **2003**, *36*, 260−267.

(22) Wertheim, M. S. *J. Stat. Phys.* **1984**, *35*, 19−34.

(23) Wertheim, M. S. *J. Stat. Phys.* **1984**, *35*, 35−47.

(24) Wertheim, M. S. *J. Stat. Phys.* **1986**, *42*, 459−476.

(25) Wertheim, M. S. *J. Stat. Phys.* **1986**, *42*, 477−492.

(26) Huang, S. H.; Radosz, M. *Ind. Eng. Chem. Res.* **1990**, *29*, 2284−2294.

(27) Hoogerbrugge, P. J.; Koelman, J. M. V. A. *Europhys. Lett.* **1992**, *92*, 155−160.

(28) Español, P.; Warren, P. *Europhys. Lett.* **1995**, *30*, 191−196.

(29) Groot, R. D.; Warren, P. B. *J. Chem. Phys.* **1997**, *107*, 4423−4435.

(30) Kranenburg, M.; Venturoli, M.; Smit, B. *J. Phys. Chem. B* **2003**, *107*, 11491−11501.

(31) Guerrault, X.; Rousseau, B.; Farago, J. *J. Chem. Phys.* **2004**, *121*, 6538−6546.

(32) Murat, M.; Kremer, K. *J. Chem. Phys.* **1998**, *108*, 4340−4348.

(33) Smith, G. D.; Paul, W. *J. Phys. Chem. A* **1998**, *102*, 1200−1208.

(34) Smith, G. D.; Borodin, O.; Paul, W. *J. Chem. Phys.* **2002**, *117*, 10350−10359.

(35) Smith, G. D.; Paul, W.; Monkenbusch, M.; Richter, D. *J. Chem. Phys.* **2001**, *114*, 4285−4288.

(36) Smith, G. D.; Borodin, O.; Bedrov, D.; Paul, W.; Qiu, X.; Ediger, M. D. *Macromolecules* **2001**, *34*, 5192−5199.

(37) Krushev, S. Computersimulationen zur Dynamik und Statik von Polybutadienschmelzen, Dissertation Thesis, Universität Mainz, 2002.

(38) Haas, F.; Hilfer, R.; Binder, K. *J. Phys. Chem.* **1996**, *100*, 15290−15300.

(39) Stadler, C.; Lange, H.; Schmid, F. *Phys. Rev. E* **1999**, *59*, 4248−4257.

(40) Stadler, C.; Schmid, F. *J. Chem. Phys.* **1999**, *110*, 9697−9705.

(41) Düchs, D.; Schmid, F. *J. Phys.: Condens. Matter* **2001**, *13*, 4853−4862.

(42) Marrink, S. J.; de Vries, A. H.; Mark, A. E. *J. Phys. Chem. B* **2004**, *108*, 750−760.

(43) Nielsen, S. O.; Lopez, C. F.; Moore, P. B.; Shelley, J. C.; Klein, M. L. *J. Phys. Chem. B* **2003**, *107*, 13911−13917.

(44) Müller, M.; Katsov, K.; Schick, M. *J. Polym. Sci.: Polym. Phys. B* **2003**, *41*, 1441−1450.

(45) Stevens, M. J. *J. Chem. Phys.* **2004**, *121*, 11942−11948.

(46) Sayar, M.; Stupp, S. I. *Macromolecules* **2001**, *34*, 7135−7139.

(47) Maiti, P. K.; Lansac, Y.; Glaser, M. A.; Clark, N. A.; Rouault, Y. *Langmuir* **2002**, *18*, 1908−1918.

(48) Srinivas, G.; Shelley, J. C.; Nielsen, S. O.; Discher, D. E.; Klein, M. L. *J. Phys. Chem. B* **2004**, *108*, 8153−8160.

(49) Binder, K.; Müller, M. *Curr. Opin. Colloid Interface Sci.* **2000**, *5*, 315−323.

(50) Yingling, Y. G.; Garrison, B. J. *J. Phys. Chem. B* **2004**, *108*, 1815−1821.

(51) Izvekov, S.; Violi, A.; Voth, G. A. *J. Phys. Chem. Lett. B* **2005**, *109*, 17019−17024.

(52) Shelley, J. C.; Shelley, M. Y.; Reeder, R. C.; Bandyopadhyay, S.; Klein, M. L. *J. Phys. Chem. B* **2001**, *105*, 4464−4470.

(53) Shelley, J. C.; Shelley, M. Y.; Reeder, R. C.; Bandyopadhyay, S.; Moore, P. B.; Klein, M. L. *J. Phys. Chem. B* **2001**, *105*, 9785−9792.

(54) Kremer, K.; Grest, G. S. *J. Chem. Phys.* **1990**, *92*, 5057−5086.

(55) Smit, B. *J. Chem. Phys.* **1992**, *96*, 8639−8640.

(56) Binder, K.; Müller, M.; Virnau, P.; MacDowell, L. G. *Adv. Polym. Sci.* **2005**, *173*, 1−104.

(57) Virnau, P.; Müller, M.; MacDowell, L. G.; Binder, K. *Comput. Phys. Comm.* **2002**, *147*, 378−381.

(58) Nielsen, S. O.; Lopez, C. F.; Srinivas, G.; Klein, M. L. *J. Chem. Phys.* **2003**, *119*, 7043−7049.

(59) Reith, D.; Meyer, H.; Müller-Plathe, F. *Macromolecules* **2001**, *34*, 2335−2345.

(60) Virnau, P.; Müller, M.; MacDowell, L. G.; Binder, K. *J. Chem. Phys.* **2004**, *121*, 2169−2179.

(61) Chen, S. S.; Kreglewski, A. *Ber. Bunsen-Ges.* **1977**, *81*, 1048−1049.

(62) Gross, J.; Sadowski, G. *Ind. Eng. Chem. Res.* **2001**, *40*, 1244−1260.

(63) Gross, J.; Sadowski, G. *Ind. Eng. Chem. Res.* **2002**, *41*, 1084−1093.

(64) Virnau, P. Monte Carlo-Simulationen zum Phasen- und Keimbildungsverhalten von Polymerlösungen, Dissertation Thesis, Universität Mainz, 2003.

(65) Yelash, L.; Müller, M.; Paul, W.; Binder, K. *J. Chem. Phys.* **2005**, *123*, 14908−15.

(66) Yelash, L.; Müller, M.; Paul, W.; Binder, K. *Phys. Chem. Chem. Phys.* **2005**, *7*, 3728−3732.

(67) Binder, K. In *Monte Carlo and Molecular Dynamics Simulations in Polymer Science*; Binder, K., Ed.; Oxford University Press: New York, 1995.

(68) Heine, D. R.; Grest, G. S.; Curro, J. C. *Adv. Polym. Sci.* **2005**, *173*, 209−249.

(69) Vettorel, T.; Meyer, H. *J. Chem. Theory Comput.* **2006**, *2*, 616−629.

CT0502099